2017 International Conference on Indoor Positioning and Indoor Navigation (IPIN), 18-21 September 2017, Sapporo, Japan

Robust WiFi-based Indoor Localization using Multipath Component Analysis

Alexandra Zayets, Eckehard Steinbach
Chair of Media Technology, Technical University of Munich, 80333 Munich, Germany.
Email: a.zayets@tum.de, eckehard.steinbach@tum.de

***Abstract*—The number of applications that rely on robust indoor localization is constantly growing. Conventional outdoor localization technologies are generally not suited for indoor use. WiFi-based indoor localization systems are a widely studied alternative since the necessary infrastructure is already available in most buildings. Existing WiFi-based localization algorithms, however, still face challenges such as high sensitivity to changes in the environment, temporal instability, a time consuming calibration process and low accuracy in non-line-of-sight (NLOS) multipath environments. In this paper, we propose a novel fingerprinting-based WiFi indoor localization scheme which operates by extracting and analyzing individual multipath propagation delays. We demonstrate through simulation the robustness of the proposed algorithm to changes in the multipath environment.**

***Index Terms*—WiFi-based indoor localization, fingerprinting.**

I. Introduction

As the capabilities of mobile devices and the indoor data communication infrastructure advance, the application possibilities and potential of Indoor Localization Systems (ILS) grow. Example applications of indoor localization include user localization in public buildings, such as shopping malls and airports, or the localization of industrial equipment in production sites and warehouses [1]. Unfortunately, conventional outdoor localization technologies are mostly unsuitable for indoor use. The work in [2] illustrates the attenuation Global Positioning System (GPS) signals undergo in an indoor environment and discusses the problems faced when trying to utilize these signals for indoor localization.

To date, various technologies have been proposed that can locate receivers in an indoor environment. This includes ILS using cameras, infrared signals, magnetic fields and sound [1].

WiFi-based ILSs come with the advantage that in most indoor environments, no additional infrastructure needs to be installed. Most buildings are already equipped with multiple WiFi access points (APs) and most portable devices have a built-in WiFi module [1]. Most existing WiFi-based localization algorithms are categorised into two groups - trilateration/triangulation and fingerprinting. Trilateration and triangulation-based algorithms estimate the distances to the APs by measuring the time-of-flight or angle-of-arrival of a signal [3], [4]. However, they only reliably work in a line-of-sight (LOS) environment. Also, since WiFi signals propagate with the speed of light [1], even tiny measurement or synchronization errors can result in localization errors up to tens of meters. Fingerprinting-based ILS as discussed in [5] - [9] measure a WiFi fingerprint in multiple locations to create a fingerprint map. A device attempting to localize itself matches its own measurements to the fingerprint map. Although to date, these methods are the most prominent in literature, they still suffer from several drawbacks, such as high sensitivity to changes in the environment, e.g. movement of people and opening of doors. Furthermore, map construction is a time-consuming process which is repeated whenever structural changes occur in the environment. Lastly, the most commonly used fingerprint, i.e., the Received Signal Strength Indicator (RSSI), tends to fluctuate significantly over time [8].

978-1-5090-6299-7/17/$31.00

In this paper we propose a WiFi fingerprinting-based indoor localization scheme which operates by extracting and analyzing individual multipath propagation delays. The proposed algorithm utilizes the signal's multipath delay profile (MDP) which is more stable over time then the RSSI. We demonstrate the robustness of the proposed system to changes in the environment through simulation.

The main contributions of this paper are the design of a novel type of WiFi MDP-based fingerprints and the development of the multipath component analysis (MCA) localization algorithm. To the best of our knowledge, the presented localization technique is the first one to utilize the MDP of a received signal as a fingerprint.

The paper is organized as follows: Section II describes the WiFi channel models referred to in this paper. Existing WiFi-based localization approaches are reviewed in Section III. The proposed algorithm is presented in Section IV. Section V presents the applied simulation methodology and the obtained results. Section VI contains an additional discussion about the proposed simulation method and future prospects.

In this paper the following notation is used. Non-bold characters represent scalar values and random variables, bold italic characters represent vectors, bold non-italic capital letters represent sets. For simplicity, we refer to a hand held device as a receiver and an AP as a transmitter.

II. Signal Propagation Properties

WiFi systems transmit data over an OFDM modulated Electromagnetic (EM) wave, generated according to the IEEE 802.11 standard. The physical behavior of a propagating EM wave is very complex and is a superposition of numerous effects and phenomena. However, keeping localization in

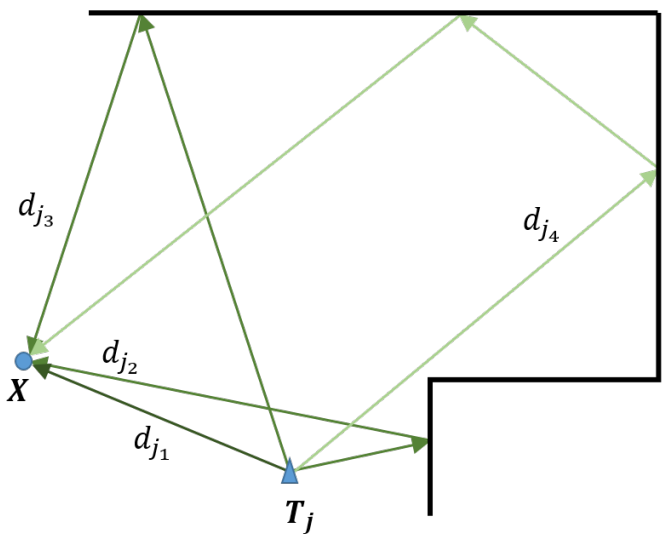

Fig. 1: Multipath signal propagation. The received signal at $\boldsymbol{X}$ is composed of a sum of multiple delayed and attenuated copies of the original signal transmitted at $\boldsymbol{T_j}$.

Notation	
M	Number of Transmitters
N	Number of MDPs stored in the fingerprint map
$\boldsymbol{T_j}$	Transmitter, $j = 1..M$
$\boldsymbol{Y_i}$	Point in the fingerprint map, $i = 1...N$
$\boldsymbol{X}$	Unknown location of the receiver in the online phase of the localization scheme
$\mathbf{F_i} = \{\boldsymbol{f_1}, ..., \boldsymbol{f_M}\}$	MDP stored with the point $\boldsymbol{Y_i}$ in the fingerprint map
$\boldsymbol{f_{ij}} = [f_{ij1}, ..., f_{ijK}]$	Vector in $\mathbf{F_i}$ that corresponds to $\boldsymbol{T_j}$
$f_{ij1}, ..., f_{ijK}$	Lengths of the signal propagation paths from $\boldsymbol{T_j}$ to $\boldsymbol{Y_i}$
f_l	Element of the vector $\boldsymbol{f_{ij}}$ that is closest to the value d_{j1}
$\mathbf{D} = \{\boldsymbol{d_1}, ..., \boldsymbol{d_M}\}$	MDP measured in the online phase
$\boldsymbol{d_j} = [d_{j1}, ..., d_{jK}]$	Vector in $\mathbf{D}$ that corresponds to $\boldsymbol{T_j}$
$d_{j1}, ..., d_{jK}$	Lengths of the signal propagation paths from $\boldsymbol{T_j}$ to $\boldsymbol{X}$
d_{jl}	Element of the vector $\boldsymbol{d_j}$ selected at the l-th iteration of the fingerprint matching algorithm
$\mathbf{L}$	A set of all indexes l for which $\exists f_l \in \boldsymbol{f_{ij}}$. $\lvert d_{jl} - f_l \rvert \to min$ and $\lvert d_{jl} - f_l \rvert < \varepsilon$
ε	Similarity threshold
$\gamma(\mathbf{D}, \mathbf{F_i} \lvert \boldsymbol{T_j})$	Similarity metric between two fingerprints $\mathbf{D}$ and $\mathbf{F_i}$ calculated for transmitter $\boldsymbol{T_j}$
$\gamma(\mathbf{D}, \mathbf{F_i})$	Similarity metric between two fingerprints $\mathbf{D}$ and $\mathbf{F_i}$

TABLE I: Notation used in the paper

mind, the indoor behavior of a propagating signal is commonly modeled in one of the two following ways [1].

A. RSSI

The RSSI is a numerical value that is easily available at the receiver. It is the received power in dB of a signal that is averaged over a certain sampling period [1]. One of the most commonly used models for the RSSI is [10]:

$$RSSI(d) = P_T - P_{d_0} - 10 \cdot \eta \cdot log_{10}\frac{d}{d_0} + X_\sigma \qquad (1)$$

where RSSI is in dB, d is the distance from the transmitter, P_T is the transmit power, P_{d_0} is the signal power at a distance d_0, η is the pass loss exponent and X_σ represents Gaussian random noise with variance σ^2.

Even though the RSSI can be modeled in various ways, it is a physical value which varies with the location of the receiver and the environment. The RSSI pattern from several transmitters is often unique to a location. Both these facts make the RSSI a popular input data source for localization.

B. Multipath Propagation Model

As an EM wave propagates with the speed of light, the distance a signal travels corresponds to a delay at the receiver. In an indoor scenario, the signal will be reflected multiple times from the walls, floors, ceilings and objects before it reaches the receiver (see Fig. 1). As a result, the received signal $r(t)$ will be composed of multiple delayed and attenuated copies of the original signal $s(t)$ summed up at the receiver.

$$r(t) = \sum_k a_k s(t - \tau_k) + z(t), \qquad (2)$$

where a_k is the attenuation undergone by the signal along the k-th path from the transmitter to the receiver and τ_k is the delay. The term $z(t)$ represents random noise added to the signal at the receiver [1]. With $\tau_k = d_k/c$, we obtain

$$r(t) = \sum_k a_k s(t - d_k/c) + z(t), \qquad (3)$$

where d_k is the length of the path traveled by the signal and c is the speed of light. The equation above represents a wide-band model and therefore can be used to obtain the response to any transmitted signal [11].

III. Existing WLAN-based localization strategies and methods

A. Trilateration and Triangulation

This type of localization algorithms is based on measuring the distances to at least 3 or 4 APs with known locations. Once the distances have been estimated, the receivers' location can be calculated using trilateration, triangulation or multi-lateration. The propagation distances are generally obtained by measuring the absolute or relative time-of-flight values between the receivers and APs in the system [1]. However, these schemes face the following challenges. Signal propagation time needs to be measured with extreme accuracy. This generally requires very precise synchronization between the receiver and transmitter. Since an EM wave propagates with the speed of light, a measurement error of 1 μs alters the calculated propagation distance by 300 m. Furthermore, accurate time-of-flight measurements are not easily available through the 802.11 standard. Very often nonstandard hardware modifications are required [1]. Lastly, these methods can only be used in LOS conditions.

Nevertheless, some of the challenges can be overcome. For example, [3] proposes a method that can increase the accuracy

of signal time-of-flight measurements through sending a predefined message multiple times to assist estimation. According to the authors, the proposed method does not require hardware modification. The ILS proposed in [3] combines angle-of-arrival and time-of-flight measurements and achieves up to 1 m accuracy in simulation results. The work in [4] uses the Time-Reversal technique to obtain more accurate distance measurements between the receiver and the transmitter. However, no matter how accurate time-of-flight measurements can become, these algorithms still require LOS conditions which are not always fulfilled in an indoor scenario.

B. Fingerprinting

Fingerprinting-based indoor localization algorithms are currently the most popular class of algorithms in the literature as their performance is not affected by NLOS conditions [1]. The localization is a two step process. Initially WiFi measurements are collected on a predefined grid in the indoor environment. The measured data is stored in a map. This is called the *offline* or *training phase*. Then, in the *online* or *run-time phase*, a receiver performs WiFi measurements and matches them to the map from Step 1.

Reference [6] gives a detailed overview of fingerprinting-based WiFi localization. The RSSI described in Section II-A is measured by default by many mobile devices and is most commonly used as a fingerprint.

In the online phase, the measured fingerprint is compared to the map. A scalar value is computed that represents the similarity between two fingerprints. Reference [6] lists several types of distance metrics which are currently used in fingerprinting-based localization. The simplest metric is the Euclidean distance between two fingerprint vectors. In the last phase of the fingerprinting procedure the algorithm selects k fingerprints in the map that are closest to the measured data. The final estimated location is computed as a weighted or unweighted average of the locations of the k fingerprints from the training data considered to be the best matches. This is referred to as the k-Nearest-Neighbors (kNN) method [6]. Measurement results from [6] show a mean localization error from 2 m to over 10 m depending on the algorithm implementation and the indoor environment.

1) Calibration and Maintenance Effort: The construction of the fingerprint map is time consuming and the map needs to be recomputed every time structural changes occur in the environment [8]. One possible solution to this problem is an approach, where the fingerprint map is constantly updated by the data received by the users of the localization system [5] [12]. The system tracks the user displacement and direction of movement and fuses that information together with the current and previous reported locations to update the fingerprint map. These approaches can, however, only be used for certain environments. The system must have a large number of users who are able to report their location. This approach cannot be used in a system with strict privacy requirements.

2) Temporal Variations of the Channel: Due to the movement of people and objects or the opening and closing of doors, the channel between a receiver and a transmitter will not remain constant over time. In [11] the author provides measurements and experimental data on temporal variations of indoor channels. The influence of the presence of people on a RSSI fingerprinting-based localization system is experimentally measured in [13]. The results show that the presence of people can increase the localization error by 11% on average and by as much as 50% in corridors.

In addition, some APs, including equipment from vendors such as Netgear, Cisco and Aruba Networks, can monitor the signal propagation environment and automatically adjust their transmit power to optimize overall network performance [8]. To overcome temporal channel variations [8] proposes a fingerprinting-based localization system that relies on the RSSI gradient and not its absolute value. This approach, however, cannot account for global changes in the environment.

3) Channel State Information (CSI)-based Fingerprinting Approaches: The RSSI is not the only signal parameter used for fingerprinting. Many recent publications use the channel state information (CSI) to construct multipath-based fingerprints. The localization schemes presented in [7] and [14] use the Channel Frequency Response (CFR) as a location fingerprint. In [7] the CFR is acquired through frequency hopping over a multitude of frequency bands. In the online phase, the time reversal technique is used to compare the measured fingerprint to the map. The experimental results in [7] demonstrate that the localization algorithm can achieve an accuracy of up to 1-2 cm in a NLOS environment. However, in the experiments the fingerprints are collected with a resolution of 5 cm which is extremely time consuming and impractical in a real system. The work in [9] extends the algorithm to multiple-input-multiple-output (MIMO) WiFi systems. In both of the localization schemes above, the complete channel information is included in the similarity metric.

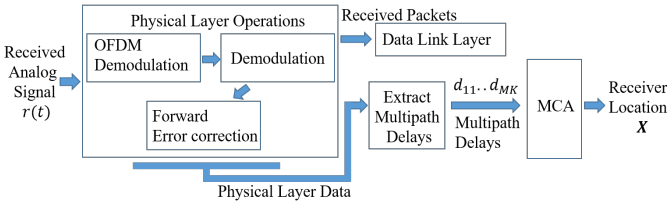

Fig. 2: The system model used for the MCA algorithm. The proposed localization scheme is composed of two main parts. The multipath delays are extracted from the physical layer data [15]. Afterwards, the multipath component analysis (MCA) algorithm is used to calculate the location of a receiver.

IV. Proposed Approach - Multipath Component Analysis

In the previous sections, the common challenges faced by WiFi-based ILSs were discussed. To overcome these challenges, we propose a novel localization scheme that uses the multipath delay profile (MDP) of a received signal as a fingerprint. To the best of our knowledge, the MDP has not

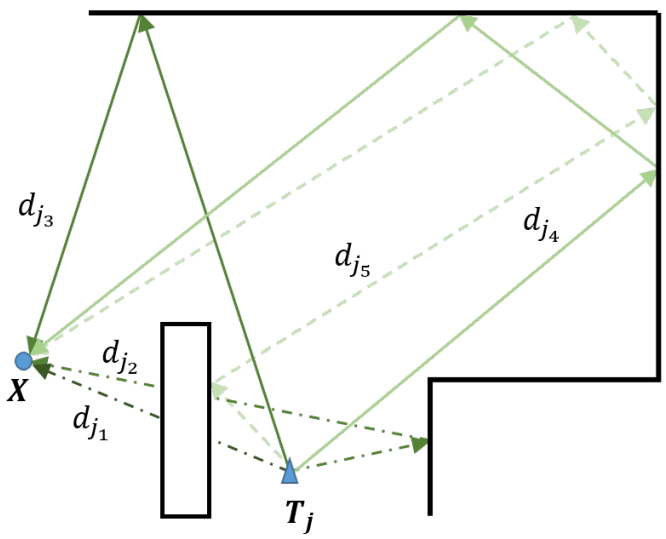

Fig. 3: An obstacle alters the MDP from Fig. 1. It blocks paths d_{j1} and d_{j2} and creates a new path d_{j5}. However, paths d_{j3} and d_{j4} can still be used to perform localization with the proposed MCA algorithm.

Algorithm 1: MCA Localization Algorithm

Data: Measured multipath delay profile
$\mathbf{D} = \{\boldsymbol{d_j}\}, j = 1..M$
transmitters $\{\boldsymbol{T_j}\}, j = 1..M$
fingerprint map $\mathbf{MAP} = \{(\boldsymbol{Y_i}, \mathbf{F_i})\}, i = 1..N$
Parameters: Similarity threshold ε
Result: $\boldsymbol{X}$- Location of the receiver

```
for ∀Y_i in the fingerprint map do
    for ∀ transmitter T_j do
        f_ij ← F_i(j)
        for ∀d_jl ∈ d_j do
            f_l ← argmin_{f_l ∈ f_ij} |d_jl − f_l|
            if |d_jl − f_l| < ε then
                γ(D, F_i|T_j) ← +(ε − |d_jl − f_l|)^2
            end
        end
    end
end
i ← argmax_i Σ_j γ(D, F_i|T_j)
X ← Y_i
```

been used before as a fingerprint for WiFi-based localization. The RSSI values fluctuate over time, and these fluctuations are the superposition of multiple effects, i.e., movement of multiple objects, variations in the signal transmit power, etc. However, the propagation path lengths shown in Fig. 1 cannot fluctuate, as they are tied to physical distances. Since the MDP measures the signal propagation distances and not power, it is also less affected by the material properties of the environment. Individual propagation paths can be blocked and new paths can appear as objects move around in the indoor environment. As illustrated by Fig. 3, even if some of the multipath components are affected by an obstacle or a change in the environment, the rest can still be used to perform precise localization. This makes the MDP a more robust fingerprint then the RSSI. The proposed localization scheme is composed of two main parts. In the system model shown in Fig. 2, the multipath delays are extracted from the physical layer data [15]. After the multipath delays have been extracted, the multipath component analysis (MCA) algorithm is used to calculate the location of a receiver.

A. Multipath Delay Profile

In the scenario presented, the indoor localization system contains M transmitters. The transmitters are labeled $\boldsymbol{T_j}$ with $j = 1...M$. In the off-line phase of the localization scheme, the multipath delay profile (MDP) is measured at N locations, i.e., $\boldsymbol{Y_i}$ with $i = 1...N$, in the indoor environment. The MDP that corresponds to the location $\boldsymbol{Y_i}$ is labeled $\mathbf{F_i}$. The pairs $(\boldsymbol{Y_i}, \mathbf{F_i})$ are then stored to a map. In the online phase, the receiver measures the MDP, $\mathbf{D}$, at an unknown location $\boldsymbol{X}$.

A multipath delay profile (MDP) is a set of vectors. The MDPs $\mathbf{F_i} = \{\boldsymbol{f_1}, .., \boldsymbol{f_M}\}$ with $i = 1...N$ are measured in the offline phase and the MDP $\mathbf{D} = \{\boldsymbol{d_1}, ..., \boldsymbol{d_M}\}$ is observed in the online phase of the localization algorithm. Each vector in a MDP contains the propagation path lengths for one transmitter. The vector $\boldsymbol{d_j} = [d_{j1}, .., d_{jK}]$ contains the length of the different path a signal can travel from the transmitter $\boldsymbol{T_j}$ to the receiver located at point $\boldsymbol{X}$. An example MDP $\{[d_{j1}, .., d_{j4}]\}$ is shown in Fig. 1. The variables and notation used in this paper are summarized in Table I.

B. Extracting the Multipath Components

In a practical scenario, the applicable MDP extraction method depends on the used hardware. The MDP extraction will vary depending on which signal data can be accessed by the localization algorithm. A custom receiver mounted on a robot can perform precise channel estimation. Extracting the multipath propagation delays from a known channel is straightforward [10]. Equation 3 calculates the received signal in a multipath environment. It can be rewritten as

$$r(t) = s(t) * h(t) + z(t) \tag{4}$$

where $s(t)$ is the transmitted signal and $h(t)$ is the impulse response of the channel between the receiver and transmitter. The term $z(t)$ represents random noise added to the signal at the receiver. A basic channel impulse response (CIR) of a multipath channel between a receiver at point $\boldsymbol{X}$ and a transmitter $\boldsymbol{T_j}$ can be written as [16]:

$$h(t) = \sum_k a_{jk}\delta(t - d_{jk}/c) \tag{5}$$

where d_{jk} is the length of one path traveled by the signal from $\boldsymbol{T_j}$ to $\boldsymbol{X}$, a_{jk} is the attenuation of the path, $\delta(t)$ is the Dirac delta function and c is the speed of light. It can be seen from

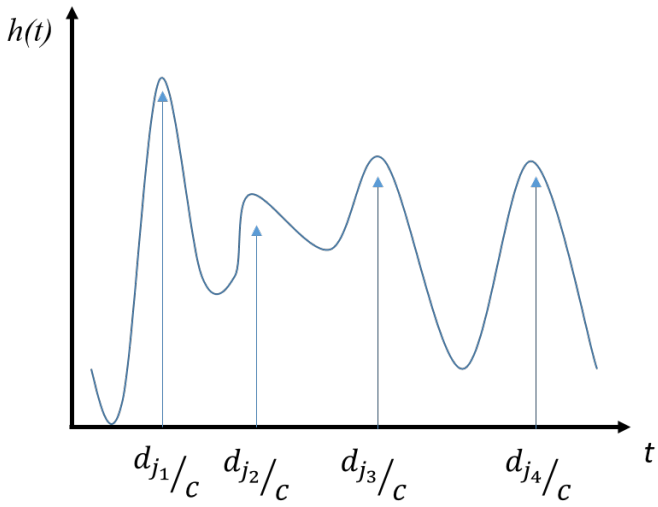

Fig. 4: The multipath delays can be identified as the peaks in a channel impulse response [10].

Eq. 5 that the multipath delays can be identified as peaks in the CIR. This is illustrated in Fig. 4.

Multipath delay extraction on mobile Android and Apple devices becomes more difficult. It is further discussed in Section VI.

C. MCA Localization Algorithm

The multipath component analysis (MCA)-based localization method is summarized in Algorithm 1. The MCA is a novel fingerprinting-based algorithm, which uses the multipath delay profile (MDP) as a fingerprint. In the off-line phase of the localization scheme, the MDP is measured for multiple points in an indoor environment to create the fingerprint map.

In the online phase, a similarity metric γ is computed between the measured MDP and the MDPs stored in the fingerprint map. The point on the map, which corresponds to the highest similarity metric is picked as the receiver's location. $\gamma(\mathbf{D}, \mathbf{F_i})$ is the similarity metric between a measured MDP - $\mathbf{D}$, and $\mathbf{F_i}$, a MDP from the fingerprint map. $\gamma(\mathbf{D}, \mathbf{F_i})$ is the sum of partial similarity metrics calculated for every transmitter.

$$\gamma(\mathbf{D}, \mathbf{F_i}) = \sum_{j=1}^{M} \gamma(\mathbf{D}, \mathbf{F_i}|\boldsymbol{T_j}) \tag{6}$$

Let $\boldsymbol{d_j}$ be the vector in $\mathbf{D}$ that contains the propagation path lengths from $\boldsymbol{X}$ to the transmitter $\boldsymbol{T_j}$. Let $\boldsymbol{f_{ij}} \in \mathbf{F_i}$ also correspond to $\boldsymbol{T_j}$. The similarity metric $\gamma(\mathbf{D}, \mathbf{F_i}|\boldsymbol{T_j})$ is calculated from $\boldsymbol{d_j}$ and $\boldsymbol{f_{ij}}$. For every delay value $d_{jl} \in \boldsymbol{d_j}$, a best match value $f_l \in \boldsymbol{f_{ij}}$ is selected such that $|d_{jl} - f_l|$ is minimal. If $|d_{jl} - f_l|$ is less then a threshold value ε, the path lengths d_{jl} and f_l are considered matched. In that case, l is added to the set $\mathbf{L}$ and a term $(\varepsilon - |d_{jl} - f_l|)^2$ is added to the similarity metric. Thus, the partial similarity metric is calculated as:

$$\gamma(\mathbf{D}, \mathbf{F_i}|\boldsymbol{T_j}) = \sum_{l \in \mathbf{L}} (\varepsilon - |d_{jl} - f_l|)^2 \tag{7}$$

$$\mathbf{L} = \{l | \exists f_l \in \boldsymbol{f_{ij}} : |d_{jl} - f_l| \rightarrow min \cap |d_{jl} - f_l| < \varepsilon\} \tag{8}$$

where ε is a similarity threshold, $d_{jl} \in \boldsymbol{d_j}$, $f \in \boldsymbol{f_{ij}}$. The threshold value ε is chosen empirically based on the input data of the algorithm. The similarity metric is designed to be higher in magnitude when more matched pairs (d_{jl}, f_l), that satisfy the above conditions, are found. The smaller the differences $|d_{jl} - f_l|$ between the matched propagation distances are, the higher the magnitude of the similarity metric will be.

V. Simulation Results

As discussed in Sections IV-B and VI, in a practical scenario the MDP extraction method primarily depends on the used hardware. Therefore, practical MDP extraction is not simulated in this paper. We use a ray-tracing approach to precisely calculate the MDPs in a known 3D indoor geometry. The performance of several localization algorithms is then simulated based on the calculated MDPs. The possible errors that can occur in a practical scenario during the MDP extraction are added to the simulation as AWGN noise.

A. Simulation Input and Output

The indoor geometry is represented by a set of bounded planes. The planes model the walls, ceilings and objects in the room. The geometry used in the paper is shown in Fig. 5a. Transmitters were placed at several points in the indoor geometry as depicted in Fig. 5b. The MDPs were then extracted at the receivers placed on every point on the grid in Fig. 5b. The lengths of the signal propagation paths of the MDPs were precisely calculated using a ray-tracing approach. The MDPs were calculated 2 times - in the off-line and online localization phases. First, the off-line phase of the localization schemes was simulated. The MDPs were calculated from the geometry without obstacles (colored in green in Fig. 5a). They were then stored to a fingerprint map. We will refer to these MDPs as reference MDPs. In the online phase the obstacles colored blue in Fig. 5a were added to the geometry. The MDPs were again calculated at the same locations. We will refer to these MDPs as query MDPs. For simplicity we will refer to the receiver locations in the simulation as query points.

B. Assumptions and Approximations

During the simulation the following approximations are made.

- The signal is treated as a broadband signal and the wave propagation and reflections are considered to be frequency independent.
- Wave phenomena such as interference and diffraction are currently neglected.
- All the surfaces in the simulation are considered planar.
- All the receivers and transmitters are considered stationary or moving at speeds low enough that signal changes due to the Doppler effects can be neglected.

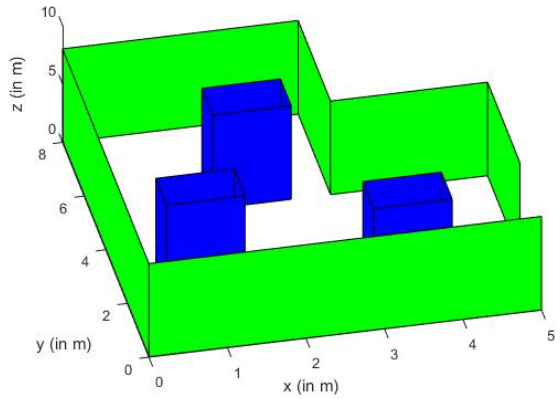

(a) The geometry of an indoor scene is represented by planes (floor and ceiling planes not displayed). The geometry used for generating the fingerprint maps is colored in green. The obstacles are the three blue columns from the floor to the ceiling. The obstacles are only included in the geometry in the online phase of the localization scheme.

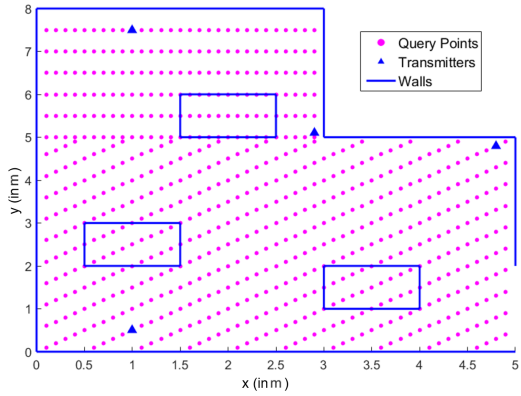

(b) Transmitter and receiver locations. The receivers, referred to as query points, are placed on every point of the grid.

Fig. 5: The inputs to the simulation are a set of planes representing the walls, ceilings and objects in the room, the locations of the transmitters and the receivers.

- No information is known about how the multipath components were extracted in the first part of the algorithm in Section IV.

C. Dealing with measurement Errors and Noise

In a practical implementation the extracted multipath delay values will deviate from the actual MDP due to:

- Computational errors due to the extraction of multipath components;
- Additive White Gaussian (AWGN) noise at the receiver;
- Scattering of the signal due to the curvature and material properties of the walls and objects.

Some of the noise components can be easily modeled. The behavior and characteristics of others can not be predicted as easily. Due to the number and variety of noise sources, the unpredictability of some of them and the overall lack of information, AWGN noise is assumed in the system. Initially, in Section V-D the localization algorithms are simulated without noise. Afterwards, in the simulation in Section V-E, AWGN noise is added directly to the multipath propagation path lengths $d_{j_1}, ..., d_{j_K}$.

D. Algorithm Comparisons

Three localization algorithms were applied to the calculated MDPs - MCA, trilateration and 'simple fingerprinting'. In this part of the simulation, no noise was added to the MDPs. A localization error was calculated for each query point. The localization errors are plotted in Fig.6a. In the top row of diagrams, the color of the query points represents the localization error calculated at those points. The localization errors at points colored in dark green are small, below $1-2m$. Localization errors at points colored in bright yellow are above $8m$. The bottom row of Fig. 6a contains histograms obtained from the localization errors for each algorithm.

The diagrams in the leftmost column in Fig. 6a illustrate the performance of localization through trilateration. Signal propagation distances were calculated between the transmitters and the query points. We refer to them as 'simulation distances'. The distances were calculated as the shortest path length in the query MDPs. Under LOS conditions this value is equal to the distance between the transmitter and the query point. Under NLOS conditions the smallest distance value in the MDP will correspond to the propagation delay that can be measured through time-of-flight by the receiver. Afterwards, a mean distance error was calculated for each query point. It was calculated as the mean of the differences between the simulation distances and the Euclidean distances between the transmitters and the query point. If the distances from a receiver to several transmitters are known, different methods can be used calculate the receivers location. Therefore, to generalize, we used the mean distance error to represent the localization error for each query point. The simulation results show several regions with points colored in dark green, i.e., with low localization errors. In those regions LOS conditions existed to all transmitters. However the area of these regions is small and the majority of the geometry is 'shadowed' by the three obstacles.

The diagrams in the middle column of Fig. 6a correspond to the localization algorithm refereed to as 'simple fingerprinting'. For each query point a channel impulse response (CIR) $h(t)$ was calculated from the reference MDPs using Eq. 5 (the attenuation factors a_k were neglected). The calculated CIRs $h(t)$ were used as fingerprints. In the online phase of the localization algorithm, a CIR $h(t)$ was calculated for each query point from the query MDPs. The calculated CIR is then compared to the fingerprint map using cross-correlation. The point to which the 'best matching' fingerprint corresponds, was picked as the calculated location of the query point. The localization error was calculated as the Euclidean distance between the calculated location and the actual coordinates of each query point. The localization errors which are above $10m$ in the

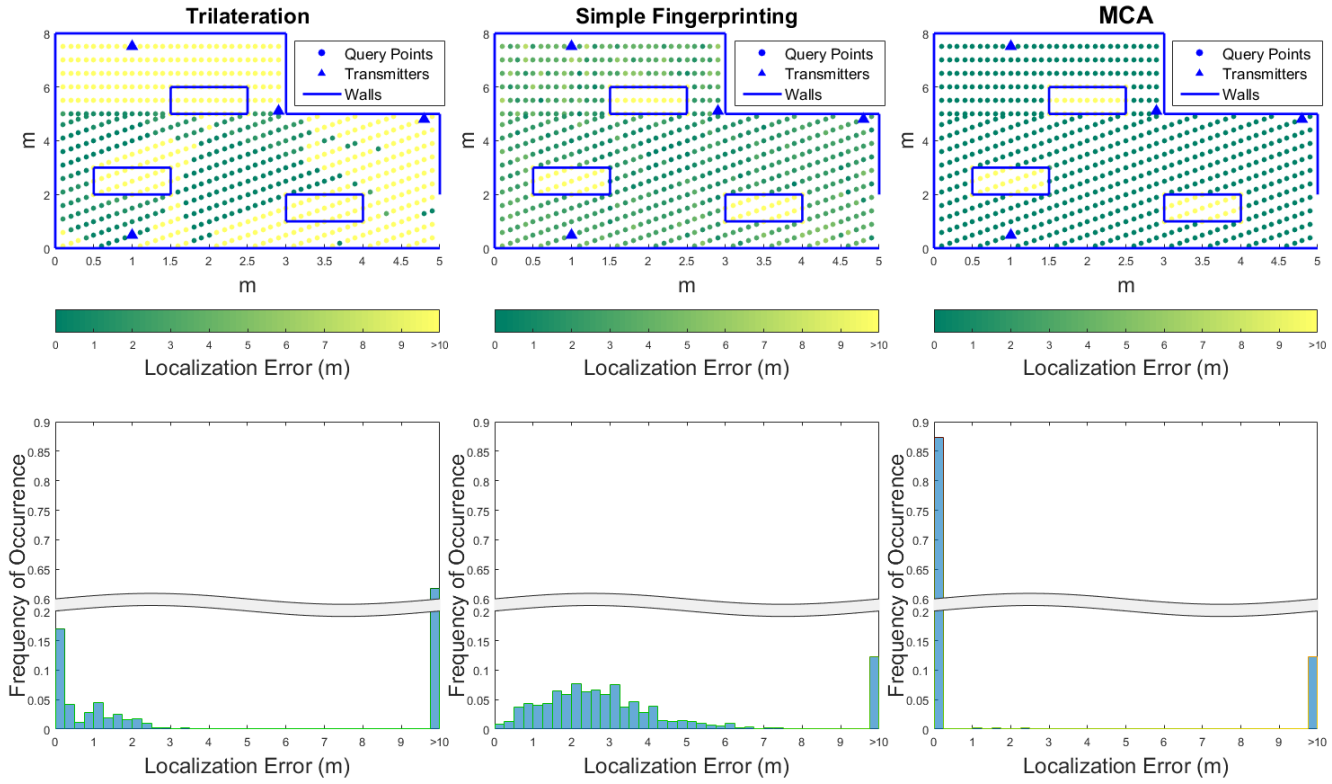

(a) Left: trilateration. Middle: 'simple fingerprinting', the CIR is used as a fingerprint, cross-correlation is used as a comparison metric. Right: MCA. No noise is added.

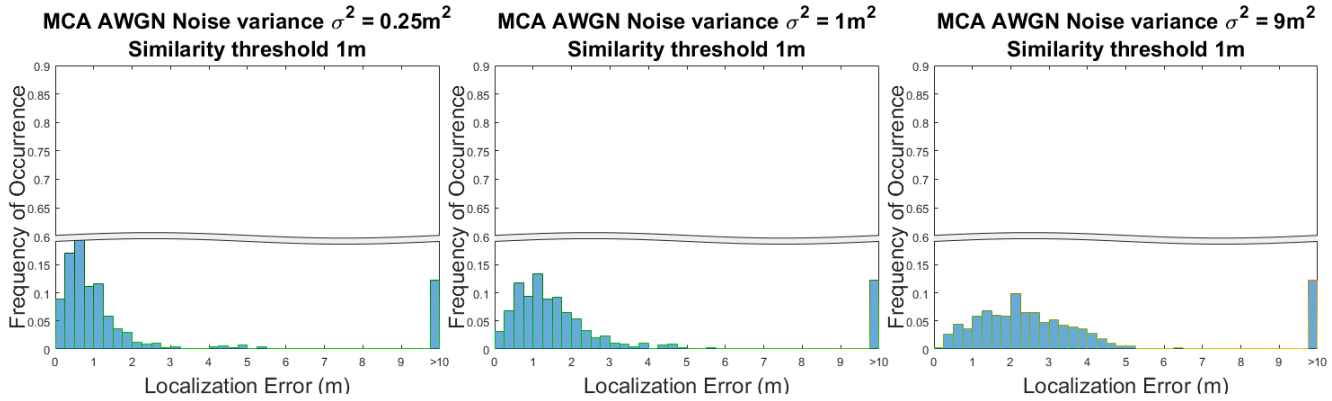

(b) AWGN noise of variance σ^2 is added to the multipath components d_{jn}.

Fig. 6: Simulation results. The color of the plotted query points indicates the localization error in m according to the shown color scale. The histograms show the frequency of occurrence of the error values (1 corresponds to a 100% occurrence rate).

histogram correspond to the points inside the obstacles. Since no signal could be received inside the obstacles, localization could not be performed. The results show that the localization algorithm is not as sensitive to the NLOS conditions. There is no obvious 'shadowing' like in the case of the diagrams on the left. However, it can be seen from the top diagram that the regions colored in dark green are the same as in the left figure, i.e., where the obstacles effected the MDPs the least. For the other points, the localization error still ranges from 0 to 5 m, with the average being around 2.5 m. This shows that if the CIR is used as a fingerprint, the localization can be performed in NLOS conditions, however localization accuracy is still influenced by changes in the environment.

The diagrams in the right column of Fig. 6a plot the localization errors obtained from the MCA algorithm presented in this paper. The similarity threshold was chosen as $1m$. The results show that localization was performed precisely for all query points, except the query points located inside the obstacles. The query points located inside the obstacles correspond to the non-zero localization errors in the histogram.

The results show that the MCA localization algorithm is the only simulated algorithm that can perform precise localization under NLOS conditions and is robust against changes in the environment.

E. Noise Resistance

The performance of the MCA algorithm was also simulated under noisy conditions. AWGN noise was added to the query MDPs. The similarity metric was set to $1m$. The variance σ^2 of the AWGN was set to $0.25m^2$, $1m^2$ and $9m^2$. Figure 6b shows the resulting error histograms. The results show that the proposed MCA algorithm still performs well in noisy conditions. However, if the variance of the noise added to the multipath components is more then $9m^2$ the localization results become unreliable.

VI. Discussion and Future Prospects

The simulation results demonstrated the robustness of the MCA localization algorithm to changes in the environment and towards the addition of noise. The proposed algorithm has the following additional advantages.

- Potential speedups for fingerprint matching.
- Privacy in indoor localization systems is becoming an increasingly larger concern [17]. Since the fingerprints are composed of a set of independent components this opens the possibility for new data protection algorithms in the localization system.
- The algorithm is well suited to be optimized through simulation. The localization algorithm is composed of two separate phases - extracting the MDP fingerprints and performing the MCA. Since they are independent, the two phases can be simulated separately. The performance of different algorithm variations can be easily objectively compared and optimized.
- The construction cost of the fingerprint map can be reduced by automatically generating part of the fingerprints through interpolation. Interpolation for MDPs has a lot of potential since individual path lengths can be interpolated separately.

One of the main challenges faced by the proposed localization scheme is the extraction of the multipath components. As mentioned in Section IV-B, one possible MDP extraction method is channel estimation. Channel estimation is very dependent on the available hardware, and is also a heavily researched topic. One example of precise channel estimation for WiFi-based indoor localization is presented in [7]. However, the current WiFi receivers in commercial portable devices such as Android and Apple phones, offer the programmer no direct access to the physical layer data. Therefore multipath delay extraction becomes more difficult. The optimal method for multipath delay extraction on commercial mobile devices is not discussed in this paper. It is the subject of our future research. Further evaluation of the system's performance is also part of our future research.

The MCA algorithm was shown in Sections V-D and V-E to be robust against changes in the environment and to noise. Multiple approaches could potentially be used to further increase the noise resistance of the algorithm. This also remains the subject of our future research.

VII. Conclusion

In this paper we discuss the common problems faced by existing WiFi-based localization algorithms and the solutions that have been presented so far. We define a novel type of WiFi fingerprint based on the multipath delay profile (MDP). In addition, we present a novel fingerprinting-based WiFi localization algorithms based on multipath component analysis (MCA). The robustness of the algorithm to environment changes is demonstrated through simulation. Simulation results that show the response of the localization algorithm to noise are also presented.

References

[1] D. R. Mautz, "Indoor Positioning Technologies," Habilitation thesis, ETH Zurich, February 2012.

[2] R. Mautz, "The challenges of indoor environments and specification on some alternative positioning systems," in *2009 6th Workshop on Positioning, Navigation and Communication*, March 2009, pp. 29–36.

[3] C. Yang and H. r. Shao, "Wifi-based indoor positioning," *IEEE Communications Magazine*, vol. 53, no. 3, pp. 150–157, March 2015.

[4] Y. Jin, N. O'Donoughue, and J. M. F. Moura, "Position location by time reversal in communication networks," in *2008 IEEE International Conference on Acoustics, Speech and Signal Processing*, March 2008, pp. 3001–3004.

[5] P. Wilk, J. Karciarz, and J. Swiatek, "Indoor radio map maintenance by automatic annotation of crowdsourced wi-fi fingerprints," in *2015 International Conference on Indoor Positioning and Indoor Navigation (IPIN)*, October 2015, pp. 1–8.

[6] F. Lemic, A. Behboodi, V. Handziski, and A. Wolisz, "Experimental decomposition of the performance of fingerprinting-based localization algorithms," in *2014 International Conference on Indoor Positioning and Indoor Navigation (IPIN)*, October 2014, pp. 355–364.

[7] C. Chen, Y. Chen, Y. Han, H. Q. Lai, and K. J. R. Liu, "Achieving centimeter-accuracy indoor localization on wifi platforms: A frequency hopping approach," *IEEE Internet of Things Journal*, vol. 4, no. 1, pp. 111–121, February 2017.

[8] Y. Shu, Y. Huang, J. Zhang, P. Cou, P. Cheng, J. Chen, and K. G. Shin, "Gradient-based fingerprinting for indoor localization and tracking," *IEEE Transactions on Industrial Electronics*, vol. 63, no. 4, pp. 2424–2433, April 2016.

[9] C. Chen, Y. Chen, Y. Han, H. Q. Lai, F. Zhang, and K. J. R. Liu, "Achieving centimeter-accuracy indoor localization on wifi platforms: A multi-antenna approach," *IEEE Internet of Things Journal*, vol. 4, no. 1, pp. 122–134, February 2017.

[10] D. Bartlet, *Essentials of Positioning and Location Technology*. Cambridge University Press, 2013.

[11] H. Hashemi, "The indoor radio propagation channel," *Proceedings of the IEEE*, vol. 81, no. 7, pp. 943–968, July 1993.

[12] J. Niu, B. Wang, L. Cheng, and J. J. P. C. Rodrigues, "Wicloc: An indoor localization system based on wifi fingerprints and crowdsourcing," in *2015 IEEE International Conference on Communications (ICC)*, June 2015, pp. 3008–3013.

[13] S. Garcia-Villalonga and A. Perez-Navarro, "Influence of human absorption of wi-fi signal in indoor positioning with wi-fi fingerprinting," in *2015 International Conference on Indoor Positioning and Indoor Navigation (IPIN)*, October 2015, pp. 1–10.

[14] K. Wu, J. Xiao, Y. Yi, D. Chen, X. Luo, and L. M. Ni, "CSI-based indoor localization," *IEEE Transactions on Parallel and Distributed Systems*, vol. 24, no. 7, pp. 1300–1309, 2013.

[15] A. Molisch, *Wireless Communications*. Wiley-IEEE Press, 2005.

[16] A. Goldsmith, *Wireless Communications*, C. U. Press, Ed., 2005.

[17] H. Li, L. Sun, H. Zhu, X. Lu, and X. Cheng, "Achieving privacy preservation in wifi fingerprint-based localization," in *IEEE INFOCOM 2014 - IEEE Conference on Computer Communications*, April 2014, pp. 2337–2345.